



Synthesis and X-ray analysis of a perfluoroalkyl-substituted azobenzene dye



Liang He^a, Harold S. Freeman^{a,*}, Monthon Nakpathom^a, Paul D. Boyle^b

^a Fiber and Polymer Science Program, North Carolina State University, Raleigh, NC 27695-8301, USA

^b Department of Chemistry, North Carolina State University, Raleigh, NC 27695-8204, USA

ARTICLE INFO

Article history:

Received 23 December 2014

Received in revised form

9 April 2015

Accepted 11 April 2015

Available online 22 April 2015

Keywords:

Perfluoroalkylazo dye

Aminoazobenzene dye

X-ray diffraction

Crystal structure

Torsion angle

Surface energy

ABSTRACT

A search for colorants capable of reducing the surface energy of synthetic fibers as well as adding color led to the synthesis and characterization of the repellency behavior of dyes such as 4-*N,N*-diethylamino-4'-tridecafluorohexylazobenzene. Unexpectedly high surface energy values and a low fluorine content on fiber surfaces then led to an interest in determining the crystal structure of this new dye. Accordingly, a single crystal was grown from acetone solution, and its structure was established using X-ray diffraction analysis. Interestingly, it was found that the azobenzene skeleton is appreciably nonplanar, having an N2–N1–C1–C2 torsion angle of 30.6°, despite the absence of substituents *ortho* to the azo bond. Further, the structure is characterized by head-to-tail molecular stacking and the *N*-ethyl groups in the molecule are positioned above the aminobenzene plane on the same side. It is likely that this combination of factors contribute to the observed surface properties of the target dye.

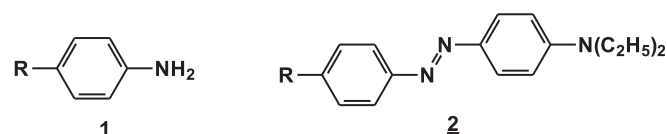
© 2015 Elsevier Ltd. All rights reserved.

1. Introduction

Our long-standing interest in arylazo compounds stems from the fact that they comprise the dominant class of synthetic colorants, are relatively easy to make, are widely used when color is sought, and their aromatic amine precursors remain of considerable interest in environmental studies. In addition, their method of synthesis opens the door to a myriad of colorants that are customized to fit specific applications. For instance, azo compounds derived from judiciously selected donor and acceptor groups can be used in non-linear optics and optical data storage [1,2]. From such studies, it is known that the optical properties obtained depend not only on the spectroscopic properties of the constituent molecules, but also on their crystallographic properties [3–5].

As part of a study aimed at designing synthetic dyes that simultaneously convey color and reduce the surface energy of natural and synthetic fibers, type **1** arylamines were used to synthesize azo dyes such as **2**. Following their application to synthetic fibers, it was found that the resultant surface energy was

surprisingly higher than expected and ESCA (Electron Spectroscopy for Chemical Analysis) experiments showed a low fluorine level on the fiber surface – despite the presence of a built-in perfluorohexyl chain. Since it was known from prior studies that dye conformations in the crystalline state influence technical performance [6] and that several recent studies have benefited from the characterization of monoazo compounds using single crystal X-ray analysis [7–12], the structural characteristics of dye **2b** were assessed using this method. While the results did not provide an unequivocal explanation for the observed surface energy properties of dye **2b**, the resultant structure was quite interesting and seemed worthwhile to report. With these points in mind, we describe here the synthesis and first crystal structure of a perfluoroalkyl-substituted azobenzene dye, namely 4-*N,N*-diethylamino-4'-tridecafluorohexylazobenzene (**2b**).



a. R = C₄F₉; b. R = C₆F₁₃

* Corresponding author.

E-mail address: harold_freeman@ncsu.edu (H.S. Freeman).

2. Experimental

2.1. General

All chemicals used in this study were purchased from either Aldrich Chemical Company or Fisher Scientific Company. Thin layer chromatography (TLC) was conducted using Whatman 250 μm silica gel 60A plates. Mass spectral data were generated using a Jeol HX110 double-focusing mass spectrometer, employing FAB(+) or ESI(+) as the ionization method, and ^1H NMR spectra were recorded on a General Electric Omega 300 MHz spectrometer using CDCl_3 as the solvent.

2.2. Synthesis of arylamines **1a–1b**

A mixture of nonafluorobutyl iodide (9.80 g, 27.8 mmol), 4-iodoaniline (5.59 g, 25 mmol), and copper bronze (5.34 g, 83.3 mmol) in DMSO (50 mL) was stirred at 120 °C for 10 h. The inorganic salts were removed by filtration, and the filtrate was diluted with H_2O (100 mL) and diethyl ether (100 mL). After stirring for 5 min, the organic layer was collected and washed five times with H_2O (100 mL) to remove DMSO and nonafluorobutyl iodide, and evaporated under reduced pressure. The mixture was distilled to give **1a** (bp 108–111 °C, 28 in Hg) as a pale yellow liquid (4.55 g, 59%). TLC: $R_f = 0.59$ (hexane:EtOAc/1:1). EI-MS m/z (rel. int.): 311 (M^+ , 31), 295 (54), 142 (100).

A mixture of 4-tridecafluorohexyl iodide (12.38 g, 27.8 mmol), 4-iodoaniline (5.59 g, 25 mmol), and copper bronze (5.34 g, 83.3 mmol) in DMSO (50 mL) was stirred at 120 °C for 10 h. Inorganic salts were removed by filtration, and the filtrate was diluted with H_2O (100 mL) and diethyl ether (100 mL). After stirring for 5 min, the organic layer was collected and washed five times with H_2O (100 mL) to remove DMSO and 4-tridecafluorohexyl iodide, and evaporated under reduced pressure. The crude product was distilled to give **1b** (bp 110–114 °C, 28 in Hg) as a pale yellow liquid (4.95 g, 48%) [13]. TLC: $R_f = 0.64$ (hexane:EtOAc/1:1). FAB-MS (positive ion) m/z (rel. int.): 412 ($\text{M} + \text{H}$, 73), 411 (M^+ , 100).

Both perfluoroalkyl-substituted arylamines were used without further characterization.

2.3. Synthesis of dyes **2a–2b**

To a stirred suspension of compound **1a** (3.11 g, 10 mmol) in 2 M HCl (15 mL) at 0–5 °C, NaNO_2 (0.71 g, 10.2 mmol) in H_2O (3 mL) was slowly added. The diazotization step was continued for 30 min and excess HNO_2 was destroyed by the addition of solid sulfamic acid. The resultant diazonium salt solution was added dropwise to *N,N*-diethylaniline (1.53 g, 10.2 mmol) dissolved in HOAc (25 mL), at a rate such that the temperature remained below 5 °C. The pH of the coupling reaction was maintained near pH 5 by the addition of solid $\text{NaOAc} \cdot 3\text{H}_2\text{O}$. The coupling step was continued for 3 h and the mixture produced was stirred overnight. The precipitate was collected by filtration, washed with H_2O , and air dried to give **2a** as an orange solid (3.49 g, 74%). $\lambda_{\text{max}}/\epsilon_{\text{max}}$ (EtOH) = 444 nm/22,300 $\text{L mol}^{-1} \text{cm}^{-1}$; TLC: $R_f = 0.82$ (hexane:EtOAc/1:1). ^1H NMR (CDCl_3): δ 1.21–1.26 (t, 6H, $J = 4.0$), δ 3.43–3.50 (q, 4H, $J = 4.0$), δ 6.71–6.74 (d, 2H, $J = 7.5$), δ 7.52–7.68 (d, 2H, $J = 7.5$), δ 7.86–7.92 (dd, 4H, $J = 8.4$). FAB-MS (positive ion) m/z (rel. int.): 472 ($\text{M} + \text{H}$, 78), 471 (M^+ , 100), 470 (36).

To a stirred suspension of compound **1b** (4.11 g, 10 mmol) in 2 M HCl (15 mL) at 0–5 °C, NaNO_2 (0.71 g, 10.2 mmol) in H_2O (3 mL) was slowly added. The diazotization step was continued for 30 min and excess HNO_2 was destroyed by adding solid sulfamic acid. The resultant diazonium salt solution was added drop wise to *N,N*-diethylaniline (1.53 g, 10.2 mmol) dissolved in HOAc (25 mL), at a

rate such that the temperature remained below 5 °C. The pH of the coupling reaction was maintained near pH 5 by the addition of solid $\text{NaOAc} \cdot 3\text{H}_2\text{O}$. The coupling step was continued for 3 h and the mixture was stirred overnight (14 h). The precipitate was collected by filtration, washed with H_2O , and air dried to give **2b** as a reddish orange solid (3.71 g, 65%). $\lambda_{\text{max}}/\epsilon_{\text{max}}$ (EtOH) = 444 nm/23,500 $\text{L mol}^{-1} \text{cm}^{-1}$; TLC: $R_f = 0.79$ (hexane:EtOAc/1:1); ^1H NMR (CDCl_3): δ 1.21–1.26 (t, 6H, $J = 4.0$ Hz), δ 3.43–3.50 (q, 4H, $J = 4.1$ Hz), δ 6.71–6.74 (d, 2H, $J = 7.54$ Hz), δ 7.65–7.69 (d, 2H, $J = 7.53$ Hz), δ 7.86–7.92 (dd, 4H, $J = 8.39$ Hz); FAB-MS (positive ion) m/z (rel. int.): 572 ($\text{M} + \text{H}$, 76), 571 (M^+ , 100); ESI-MS (+), $\text{C}_{22}\text{H}_{19}\text{F}_{13}\text{N}_3$ [$\text{M} + \text{H}$] $^+$: calcd. 572.1371, obsd. 572.1365.

2.4. X-ray analysis

X-ray quality crystals of dye **2b** were grown by slow evaporation of an acetone solution at room temperature. The selected crystal was mounted on a nylon loop using a small amount of Paratone N oil, and X-ray measurements were made on a Bruker-Nonius X8 Apex2 diffractometer at 110 K. The unit cell dimensions were determined from a symmetry constrained fit of 4145 reflections with $5.24^\circ < 2\theta < 42.22^\circ$. The data collection strategy involved the use of a number of ω and ϕ scans to collect data up to 42.32° (2θ) and the frame integration was performed using SAINT [14]. The resulting raw data was scaled and absorption corrected using a multi-scan averaging of symmetry equivalent data using SADABS [15].

The structure was solved by direct methods using the SIR92 program [16]. All non-hydrogen atoms were obtained from the initial solution and the hydrogen atoms were introduced at idealized positions and were allowed to refine isotropically. The structural model was fit to the data using full matrix least-squares based on F^2 . The calculated structure factors included corrections for anomalous dispersion from the usual tabulation. The structure was refined using the XL program from SHELXTL [17], graphic plots were produced using the NRCVAX crystallographic program suite. Crystallographic data are summarized in Table 1. These data have been deposited with the Cambridge Crystallographic Data Centre and was assigned CCDC 1057216.

2.5. Electron density calculations

Electron density calculations were conducted using PiSystems version 6.3, Copyright 2002–2013 Neutronix Software. This software allows the semi-empirical quantum-theoretical calculation of the π system of organic molecules. Values obtained from calculating electron-density alterations correspond to increase (decrease) of the negative charge at a specific atom. The values obtained have the unit number of electrons and the algebraic sum of these numbers over all π atoms is zero. Further, these values show the difference in the π -electron densities (=charge orders) between the ground and the electronically excited state at each atom of the π system, i.e. the shift of the electrons in the π system when it is electronically excited.

3. Results and discussion

3.1. Dye synthesis

The synthesis of monoazo dyes having a perfluoroalkyl chain in the diazo component is illustrated in Fig. 1. In step 1, 4-(nonafluorobutyl)aniline and 4-(tridecafluorohexyl)aniline were prepared by the reaction of 4-iodoaniline with the corresponding perfluoroalkyl iodides (RI) in the presence of copper bronze [18]. Diazotization of 4-(perfluoroalkyl)anilines (**1**) followed by coupling

Table 1
Summary of crystal data for the perfluoroalkylazobenzene dye **2b**.

Formula	C ₂₂ H ₁₈ F ₁₃ N ₃
Formula weight (g/mol)	571.39
Crystal dimensions (mm)	0.24 × 0.10 × 0.01
Crystal color and habit	Orange plate
Crystal system	Orthorhombic
Space group	P b c a
Temperature, K	110
a, Å	11.6808(6)
b, Å	9.3383(5)
c, Å	41.733(2)
α, °	90.00
β, °	90.00
γ, °	90.00
V, Å ³	4552.2(4)
Number of reflections to determine final unit cell	4145
Min and Max 2θ for cell determination, °	5.24, 42.22
Z	8
F(000)	2304
ρ (g/cm ³)	1.667
λ, Å, (MoKα)	0.71073
μ, (cm ⁻¹)	0.174
Diffractometer type	Bruker-Nonius Kappa Axis X8 Apex2
Scan type(s)	Omega and phi scans
Max 2θ for data collection, °	42.32
Measured fraction of data	0.996
Number of reflections measured	19285
Unique reflections measured	2487
R _{merge}	0.1181
Number of reflections included in refinement	2487
Cut off threshold expression	>2σ(I)
Structure refined using	full matrix least-squares using F ²
Number of parameters in least-squares	343
Min & Max peak heights on final DF Map (e ⁻ /Å)	-0.321, 0.295

Where: $R1 = \frac{\sum(|Fo| - |Fc|)}{\sum Fo}$ $wR2 = \frac{[\sum(w(Fo2 - Fc2)^2)]^{1/2}}{[\sum(w Fo4)]^{1/2}}$
 $GOF = \frac{[\sum(w(Fo2 - Fc2)^2)]}{(No. of reflns. - No. of params.)}^{1/2}$.

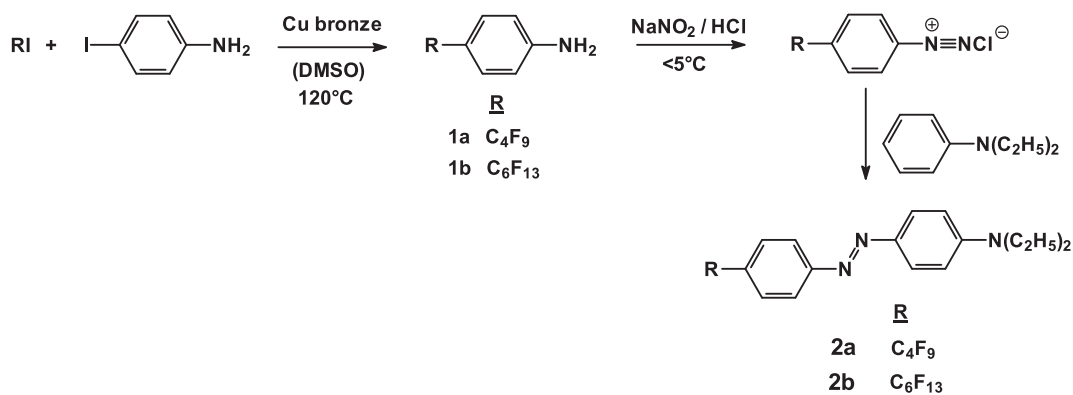


Fig. 1. Three-step synthesis of perfluoroalkyl-substituted azobenzene dyes.

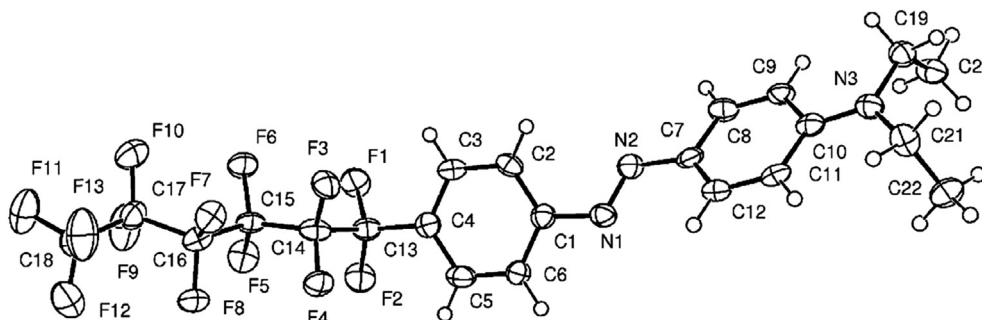


Fig. 2. ORTEP drawing of dye **1b** showing the numbering scheme. Ellipsoids are at the 50% probability level and hydrogen atoms were drawn with arbitrary radii for clarity.

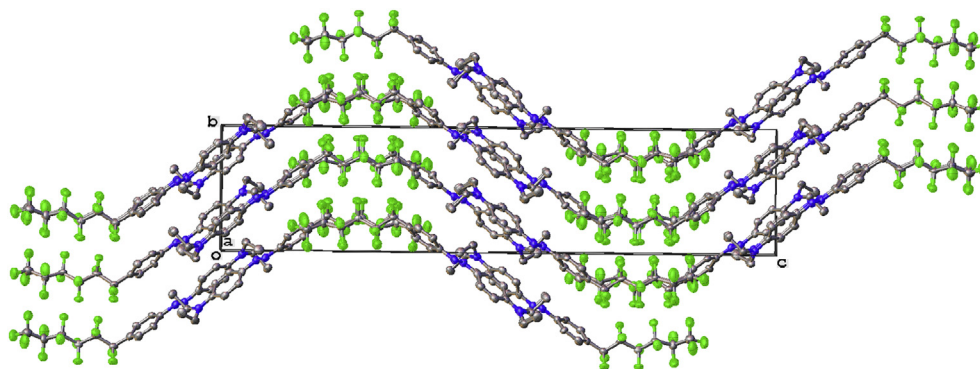


Fig. 3. Packing diagram for dye **2b** viewed along axis *b*.

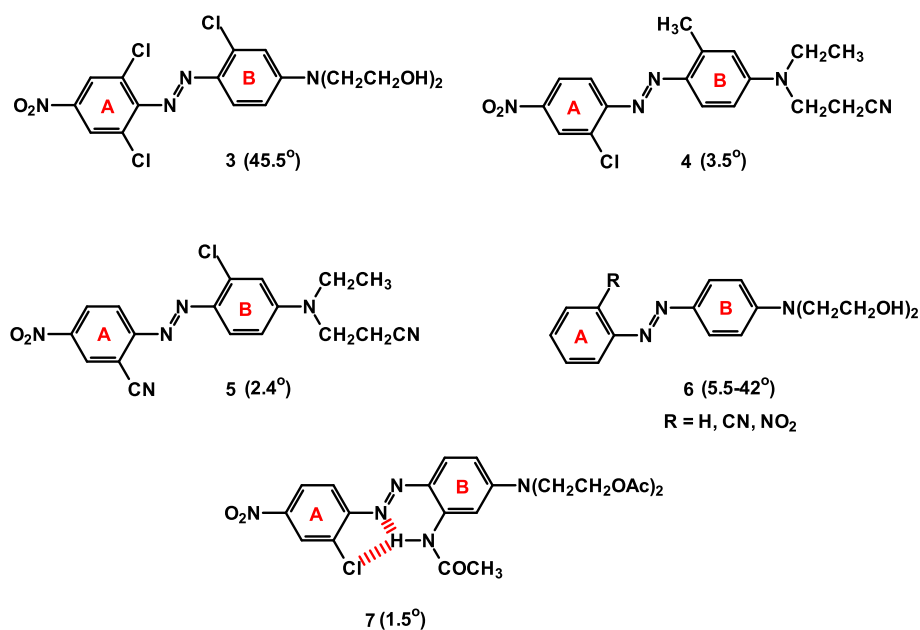


Fig. 4. Representative aminoazobenzene dye structures and their C–N–N–C torsion angles.

Table 2
Comparison of experimental torsion angles and λ_{\max} values for types **2** and **6** dyes.

Dye no.	λ_{\max} (nm)	Torsion angle ($^{\circ}$)
2b	444	30.6
6 (R = H)	413	10.3
6 (R = (CN))	458	5.5
6 (R = NO ₂)	450	42

with *N,N*-(diethyl)aniline afforded type **2** orange dyes (λ_{\max} 444 nm) in 74% (**2a**) and 65% (**2b**) yields.

3.2. X-ray analysis

The single crystal of dye **2b** obtained by evaporation of an acetone solution was found to have the orthorhombic space group

Pbca. The crystal structure and atomic numbering are given in Fig. 2 and the corresponding packing diagram is presented in Fig. 3. It is clear from Fig. 2 structure that the aminoazobenzene framework of the perfluoroalkyl-substituted dye is significantly nonplanar, with an N2–N1–C1–C2 torsion angle of 30.6°. This contrasts the various examples of monoazo hydrophobic dye structures reported in the Cambridge Crystallographic Database (CCD, 2008), where it can be seen that azobenzene compounds having bulky *ortho*-substituents are typically nonplanar [11,19], while those lacking or having small *ortho*-substituents are nearly planar (cf. Fig. 4). For example, type **3** dyes which have chlorine atoms in the 2,6-positions of the diazo component (ring A) are characterized by a large torsion angle between the two rings. Removal of one of the chlorines to give a type **4** dye, which also has a methyl group in the coupler (ring B) *ortho* to the azo group,

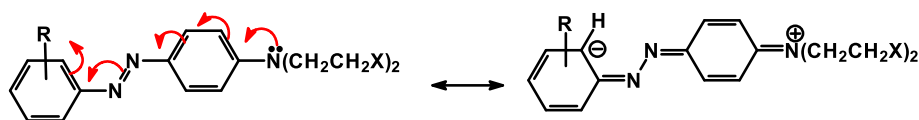
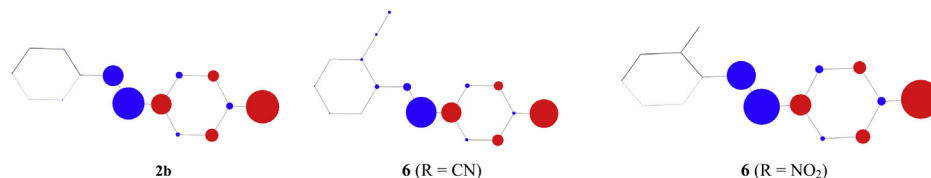


Fig. 5. Electron-delocalization essential to increasing λ_{\max} in arylazoaminobenzene dyes.

Table 3
Calculated electron density alterations upon excitation into the first excited singlet state.^a



Dye	C-4	C-3	C-2	C-1	N-1	N-2	C-7	C-8	C-9	C-10	N-3
2b	0.016	0.002	0.018	0.012	0.137	0.276	-0.173	0.053	-0.089	0.048	-0.251
6 (R = CN)	0.015	-0.002	0.029	0.044	0.075	0.265	-0.177	0.045	-0.068	0.035	-0.247
6 (R = NO ₂)	0.007	0.003	0.001	-0.010	0.227	0.281	-0.169	0.067	-0.104	0.069	-0.305

^a Red and blue circles indicate a decrease and increase in electron density, respectively. Circle sizes indicate the relative intensity of the change in electron density for a given atom. (For interpretation of the references to colour in this table legend, the reader is referred to the web version of this article.)

or replacement of the 2,6-dichloro grouping with an *ortho*-cyano group (cf. dye **5**) leads to an essentially planar azo structure. In the case of type **6** dyes, structures having R = H or CN are relatively planar, while the *ortho*-NO₂ substituted dye has a torsion angle of 42° [20–22]. When R = NO₂, loss of planarity arises from a steric interaction between the -O⁻ moiety of the NO₂ group and the azo N-atom attached to ring B. In the case of dye **7**, the presence of bifurcated H-bonding gives rise to a planar dye, a benefit of having an *ortho*-NHCOCH₃ group in the coupler along with an *ortho*-Cl group in the diazo component [7].

The packing diagram shows a head-to-tail arrangement of dye **2b** molecules in the crystal cell and Z = 8. It can be seen in Fig. 3 that two layers of dye molecules are arranged in opposite directions. In addition, dye molecules are in position to facilitate intermolecular interactions between perfluoroalkyl chains.

Regarding other key structural components of dye **2b**, the N1–N2–C7–C12 torsion angle is -13.9° and the C4–C13–C14 bond angle of 114.7°, indicating that the 4-perfluoroalkyl group is not coplanar with phenyl ring A, unlike the 4-NO₂ group of dyes such as **4–7** [5,11]. As illustrated in Table 2, this influences the λ_{max} of arylazoaminobenzene dyes. When comparing dyes **2b** and **6**, it can be seen that the order of decreasing λ_{max} is **6** (R = CN) > **6** (R = NO₂) > **2b** > **6** (R = H). This indicates both the electron delocalization power of the ring substituents (cf. Fig. 5) as well as the importance of coplanarity. Reduction in planarity and removal of the electron-withdrawing group in dyes **6** lowers λ_{max} and while the *para*-C₆F₁₃ group has a strong bathochromic effect when compared with dye **6** (R = H) its effect is less than that of the *ortho*-NO₂ group (cf. Table 2). These results are consistent with calculated values for electron density alterations arising from excitations from the ground state to the first excited singlet state (cf. Table 3). Here it can be seen that the intensity of pull of electrons into ring “A” of dye **2b** is less than that of dye **6** (R = NO₂), despite the higher torsion angle associated with the latter dye (cf. N-3, N-1, C-2, and C-4).

Bearing in mind that the low surface energy afforded by fluorocarbon-based water and oil repellents arises from the

alignment of -CF₃ groups on fiber surfaces following adsorption [23] (cf. Fig. 6), the present results suggest that the torsional twist associated with dye **2b** interfered with this normal alignment. Consequently, a higher than expected surface energy was obtained.

4. Conclusion

Single crystals of a perfluoroalkyl-substituted arylazobenzene based dye were grown from an acetone solution and its molecular structure was characterized by X-ray crystallography, providing the first X-ray structure of a monoazo dye containing a perfluoroalkyl group. It was found that the presence of a *para*-C₆F₁₃ group gives rise, unexpectedly, to an azobenzene skeleton that is quite nonplanar (θ = 30.6). In addition, the packing diagram shows that the dye molecules position themselves in a manner that promotes intermolecular interactions between perfluoroalkyl chains.

Acknowledgment

The authors wish to thank the Department of Chemistry at North Carolina State University and the State of North Carolina for funding the purchase of the Apex2 diffractometer.

References

- [1] Bach H, Anderle K, Fuhrmann T, Wendorff JH. Biphoton-induced refractive index change in 4-amino-4'-nitroazobenzene/polycarbonate. *J Phys Chem* 1996;100:4135–40.
- [2] Taniike K, Matsumoto T, Sato T, Ozaki Y, Nakashima K, Iriyama K. Spectroscopic studies on phase transitions in Langmuir-Blodgett films of an azobenzene-containing long-chain fatty acid: dependence of phase transitions on the number of monolayers and transition cycles among h-, j-, and j'-aggregates in multilayer films. *J Phys Chem* 1996;100:15508–16.
- [3] Biswas N, Umamathy S. Structures, vibrational frequencies, and normal modes of substituted azo dyes: infrared, raman, and density functional calculations. *J Phys Chem A* 2000;104:2734–45.
- [4] Willner I, Rubin S. Control of the structure and functions of biomaterials by light. *Angew Chem Int Ed* 1996;35:367–85.
- [5] He L, El-Shafei A, Freeman HS, Boyle P. X-ray and molecular modelling studies of 4-[N-alkylamino]azobenzene dyes. *Dyes Pigments* 2009;82:299–306.
- [6] McGeorge G, Harris RK, Batsanov AS, Churakov AV, Chippendale AM, Bullock JF, et al. Analysis of a solid-state conformational rearrangement using ¹⁵N NMR and X-ray crystallography. *J Phys Chem A* 1998;102:3505–13.
- [7] Freeman HS, Posey Jr JC, Singh P. X-ray crystal structure of disperse red 167. *Dyes Pigments* 1992;20:279–89.
- [8] Freeman HS, McIntosh SA, Singh P. X-ray crystal structure of disazo dyes. Part 2: derivatives of C.I. Disperse Yellow 23 and C.I. Disperse Orange 29. *Dyes Pigments* 1997;35:149–64.
- [9] Freeman HS, McIntosh SA, Singh P. X-ray crystal structure of disazo dyes. Part 1: C.I. Disperse Orange 29. *Dyes Pigments* 1997;35:11–21.
- [10] Yang W, You X-L, Zhong Y, Zhang D-C. The crystal structure of 4-[(2-methoxy-4-nitro-phenylazo)-phenyl]-dimethylamine. *Dyes Pigments* 2007;73:317–21.

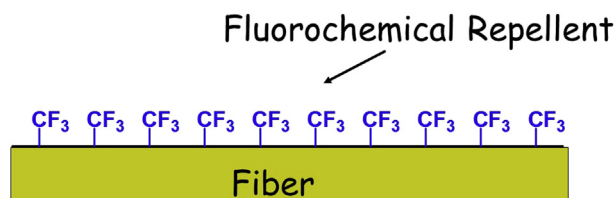


Fig. 6. Schematic representation for -CF₃ group alignment following application of a fluorocarbon repellent to a fiber surface.

- [11] Seo J, Jo WJ, Choi G, Park K-M, Lee SS, Lee JS. X-ray crystal structure of C.I. Disperse Brown 1. *Dyes Pigments* 2007;72:327–30.
- [12] Lee J-E, Kim HJ, Han MR, Lee SY, Jo WJ, Lee SS, et al. Crystal structures of C.I. Disperse red 65 and C.I. Disperse red 73. *Dyes Pigments* 2009;80:181–6.
- [13] Nakpathom Monthon. Design and synthesis of surface-active disperse dyes [Doctoral thesis]. North Carolina State University; 2002.
- [14] Bruker-Nonius. SAINT version 2008.6. Madison, WI 53711, USA: Bruker-Nonius; 2008.
- [15] Bruker-Nonius. SADABS version 2008.4. Madison, WI 53711, USA: Bruker-Nonius; 2008.
- [16] Altomare A, Cascarano G, Giacovazzo C, Guagliardi A, Burla MC, Polidori G, et al. SIRPOW.92 – a program for automatic solution of crystal structures. *J Appl Cryst* 1994;27:435–6.
- [17] Bruker-AXS. XL version 6.12, Bruker-AXS, Madison, WI 53711, USA.
- [18] Yoshino N, Kitamura M, Seto T, Shibata Y, Abe M, Ogino K. Syntheses of azobenzene derivatives having fluoroalkyl chain and their monomolecular film formation at the air/water interface. *Bull Chem Soc Jpn* 1992;65:2141–4.
- [19] Glowka ML, Olubek Z. 2'-Bromo-4-[N-(2-cyanoethyl)-N-(2-phenylethyl)] amino-4'-nitroazobenzene. *Acta Cryst* 1994;C50:458–60.
- [20] McIntosh S, Freeman HS, Singh P. X-ray crystal structure of the dyes 2-nitro-4'-[N,N-bis(β-hydroxyethyl)amino]azobenzene and 2-cyano-4'-[N,N-bis-(β-hydroxyethyl)amino]azobenzene. *Text Res J* 1989;59:389–95.
- [21] McIntosh S, Freeman HS, Singh P. X-ray crystal structure of the dye 4-[N,N-bis-(β-hydroxyethyl)amino]azobenzene. *Dyes Pigments* 1991;17:1–10.
- [22] Park K-M, Yoon I, Lee SS, Choi G, Lee JS. X-ray crystal structure of C.I. Disperse Blue 79. *Dyes Pigments* 2002;54:155–61.
- [23] Cooke TF. Fibers and textiles: an overview. In: Kelly A, editor. *Concise encyclopedia of composite materials*. New York: Elsevier Science Ltd; 1994. p. 97.